

Constraining HeII Reionization Detection Uncertainties via Fast Radio Bursts

Albert Wai Kit Lau,¹Ayan Mitra,^{2,3*} Mehdi Shafiee^{4,5,6}George Smoot^{1,4,7,8,9}

¹*Department of Physics, The Hong Kong University of Science and Technology, Clear Water Bay, Kowloon, Hong Kong*

²*School of Engineering and Digital Sciences, Nazarbayev University, Nur-Sultan, Kazakhstan*

³*Kazakh-British Technical University, Almaty, Kazakhstan*

⁴*Energetic Cosmos Laboratory, Nazarbayev University, Nur-Sultan, Kazakhstan*

⁵*Department of Physics, Engineering Physics Astronomy, Queen's University, Kingston, ON Canada*

⁶*Arthur B. McDonald Canadian Astroparticle Physics Research Institute, Queen's University, Kingston, ON Canada*

⁷*Paris Centre for Cosmological Physics, Université de Paris, CNRS, Astroparticule et Cosmologie, F-75013 Paris, France*

⁸*Physics Department and LBNL, University of California, Berkeley, CA, 94720 USA*

⁹*Institute for Advanced Study Hong Kong University of Science and Technology, Clear Water Bay, Kowloon, Hong Kong*

Accepted XXX. Received YYY; in original form ZZZ

ABSTRACT

Context. The rate of detection of Fast Radio Bursts (FRBs) in recent years has increased rapidly and getting samples of sizes $\mathcal{O}(10^2)$ to $\mathcal{O}(10^3)$ is likely possible. FRBs exhibit short radio bursts in order of milliseconds at frequencies of about 1 GHz. They are bright and have high dispersion measures which suggest they are of extra galactic origin. Their extragalactic origin allows probing the electron density in the intergalactic medium. One important consequence of this is, FRBs can help us in understanding the epoch of helium reionization.

Aims. In this project, we tried to explore the possibility of identifying the epoch of Helium II (HeII) reionization, via the observations of early FRBs in range of $z = 3$ to 4. We constrained the HeII reionization with different number of observed early FRBs and associated redshift measurement errors to them.

Methods. We build a model of FRB Dispersion Measure following the HeII reionization model, density fluctuation in large scale structure, host galaxy interstellar medium and local environment of FRB contribution. We then fit our model to the ideal inter galactic medium (IGM) dispersion measure model to check the goodness of constraining the HeII reionization via FRB measurement statistics.

Conclusion. We report our findings under two categories, accuracy in detection of HeII reionization via FRBs assuming no uncertainty in the redshift measurement and alternatively assuming a varied level of uncertainty in redshift measurement of the FRBs. We show that under the first case, a detection of $N \sim \mathcal{O}(10^2)$ FRBs give an uncertainty of $\sigma(z_{r,fit}) \sim 0.5$ from the fit model, and a detection of $N \sim \mathcal{O}(10^3)$ gives an uncertainty of $\sigma(z_{r,fit}) \sim 0.1$. While assuming a redshift uncertainty of level 5 – 20%, changes the $\sigma(z_{r,fit}) \sim 0.5$ to 0.6 in $N \sim 100$ case respectively and $\sigma(z_{r,fit}) \sim 0.1$ to 0.15 for $N \sim 1000$ case.

Key words: FRBs, HeII reionization, IGM, host galaxy electron distribution

1 INTRODUCTION

Fast radio bursts (FRBs) are a new sensation in astronomy. They were first detected in 2007 (Lorimer et al. 2007). They are radio transients of short duration. Observations show, they have high dispersion measure (DM) and high galactic latitude ($|b| > 40^\circ$) (Katz 2016) of incidence, thus confirming that they originated at cosmological distances (Jaroszynski 2019). This enables them to be used as an efficient cosmological probe. Although origin of FRBs are still not known definitively, but it is understood that they are caused by an

unknown high energy phenomena (Chatterjee et al. 2017). On the radio sky, radio transients vary according to the dynamical time. Till now only a very few FRBs observed are typically repetitive (thus ruling out any possibility of their origins from cataclysmic events) (Spitler et al. 2016; CHIME/FRB Collaboration et al. 2019a,b) and only one is detected exhibiting periodicity of 16.35 ± 0.18 days (The CHIME/FRB Collaboration et al. 2020). For short bursts, the dynamical time ranges from [0.1ms – 10ms], corresponding from a neutron star to a white dwarf respectively (Fan et al. 2002). The FRB signals possess interesting features such as:

- FRB signals have a time delay which is inversely proportional to the square of the frequency i.e. $\Delta t \propto \nu^{-2}$

* E-mail: ayan.mitra@nu.edu.kz

where ν is the radiation frequency of the burst (Wiklind & Volker Bromm 2012).

- The dependence on the frequency of the burst's width, which corresponds to Kolmogorov's power law. (Yoshizawa 1978), according to which the burst's width is proportional to ν^{-4} . Mathematically the broadened width relation is given in terms of the DM as,

$$width = 8.3 \times 10^{-3} \left(\frac{DM}{\text{pc cm}^{-3}} \right) \left(\frac{\Delta\nu}{\text{MHz}} \right) \left(\frac{\nu}{\text{GHz}} \right)^{-3} \text{ ms}, \quad (1)$$

where $\Delta\nu$ is the channel bandwidth (Hashimoto et al. 2019).

Therefore the higher the frequency, less is the time delay. This dispersion feature corresponds to cold plasma and it is predicted that the radio bursts were propagating through such cold plasma. The delay mostly happens due to scattering of the free electrons along the line of sight. This important information is thus encoded in the redshift (z) information of the FRBs. Therefore the magnitude of the integral of the electron density from the source to the observer along the line of sight of the FRB gives the measure of this dispersion called as the DM. DM is a time delay of the signal in comparison with the time the signal traveled in vacuum. The other particles does not interact as much as electrons, their influence is thus insignificant. The general expression for DM, therefore contains only the effect of electrons which is calculated as below (Lorimer et al. 2007; Deng & Zhang 2014):

$$DM = \int_0^{z'} \frac{n_e}{(1+z)} dl. \quad (2)$$

where n_e is the electron density.

The contribution of the DM by materials on a part of line of sight only from z' to z'' range is

$$DM|_{z'}^{z''} = \int_{z'}^{z''} \frac{n_e}{(1+z)} dl. \quad (3)$$

By calculating DM versus redshift, we can use FRBs as precision probes of the Universe (Li et al. 2018a) especially for studying problems like the missing baryons (Muñoz & Loeb 2018), dark energy equation of state (Zhou et al. 2014) and reionization (especially the second helium (HeII) reionization) (Linder 2020). However the available statistics of FRB at our disposal at the moment are too scarce to make elaborate cosmological estimations from them. But keeping in mind of the future detection scopes (Bandura et al. 2014), in this paper we discuss the prospect of using FRBs to investigate their potential in probing the mechanism of HeII reionization, In particular, by considering the role of anisotropy of electron distribution in host galaxy (Linder 2020).

This paper is outlined as follows : in section §2 we discuss about the epoch of reionization from the point of view of FRB study and this paper. In the next section §3, we summarize the contributions to the FRB DM from different factors. After that the remainder of the paper is focused on trying to infer the FRB statistics required for constraining the HeII reionization detection redshift, while taking into consideration realistic redshift uncertainty measurements, section (§4). In the last two sections (§5, §6), we summarize our results and provide the final inference based on our analysis.

2 HELIUM II REIONIZATION

The epoch of reionization in the history of the Universe, was when the first electrons (e^-) of the neutral hydrogen (HI) and helium (HeI) were lost (Giroux 1990; Vishniac 1987; Lidde 2003; Peacock 1999) from their outer shells. This epoch marked an important phase in the structure of the Universe rendering the intergalactic medium ionized from neutral. Substantial scientific energy has been put into understanding this process and what triggered it's epoch and it's subsequent evolution. Current constraints strongly suggests that this period occurred within a redshift range of $6 < z \sim 15$ (Barkana & Loeb 2001; Bromm & Larson 2004; Paoletti et al. 2011). Post the epoch of reionization, much later in the timeline of the Universe (around two billion years since the Big Bang), followed the second ionization of the helium ions, HeI→HeII. This transition is expected to occur around $z \sim 3$ (McQuinn et al. 2009; Worseck et al. 2011; Furlanetto & Oh 2008; Sokasian et al. 2002). This phenomenon is referred to, as the Helium reionization (HeII). However decisive observational detections are missing for the HeII transition signatures. The strongest detection comes from the far ultraviolet spectra of the HeII Ly α forest from the lines of sight to several quasars along $z \sim 3$ (McQuinn et al. 2009; Caleb et al. 2019). However, the comparatively less number of lines of sight, puts a high statistical uncertainty in the measurement of the exact time and nature of this process. There are searches to try to find other methods for identifying this transition with better precision. One of them being the study of the evolution of the temperature of the intergalactic medium around the neighbourhood of $z \sim 3$ (Caleb et al. 2019; McQuinn et al. 2009).

FRB's in this context, could be useful for studying the epoch of the HeII reionization via their DM (Caleb et al. 2019). This is because FRB's last for short instant (few milliseconds) and this enables the study of all the ionized baryons (integrated column density) along the observed line of sight in it's path.

3 DM OF FRB

The expression of DM from a FRB is given in equation (2). The total DM from a FRB however, consists of four main contributing factors, namely the DM related to the Milky Way DM_{MW} , to the Intergalactic Medium DM_{IGM} , to the host galaxy DM_{host} and to the source itself DM_{source} (Thornton et al. 2013),

$$DM = DM_{MW} + DM_{IGM} + DM_{host} + DM_{source} \quad (4)$$

However, we do not have the details of the FRB source so we have only a set of possible range for the DM_{source} (Deng & Zhang 2014). It has been extensively discussed that DM_{source} and DM_{MW} both are ignorable (Thornton et al. 2013; Schnitzeler 2012) in the overall DM budget of the FRB. In our case, the DM_{host} factor is further broken up into two constituent terms, $DM_{host} = DM_{local} + DM_{GalaxyDisk}$. Where DM_{local} is the region near the FRB in question with high star formation rate. While the term $DM_{GalaxyDisk}$ is the term contributing from the galactic disk region with the interstellar medium components.

3.1 DM Contribution by IGM

3.1.1 HeII reionization model

(Caleb et al. 2019) derived a general expression for the DM estimate from an ionized intergalactic medium. Assuming a universe of purely Helium and Hydrogen, with a Helium mass fraction of Y , the number density of free electron density is given by the following expression :

$$n_e = \frac{\rho_{c,0}\Omega_b f_{IGM}}{m_p} \left[(1-Y)\chi_{e,H}(z) + \frac{Y}{4}\chi_{e,He}(z) \right] (1+z)^3 \quad (5)$$

where $\rho_{c,0}$ is the critical mass density at $z = 0$, f_{IGM} is the fraction of the baryon mass in the IGM (to a first order approximation (Fukugita et al. 1998; Shull et al. 2012) showed this can be approximated to $f_{IGM} = 0.83$). m_p refers to the mass of proton. Y refers to the Helium mass fraction, which is measured to be 0.243 by Planck. Ω_b is the current baryon mass fraction of the Universe. $\chi_{e,H}(z)$, $\chi_{e,He}(z)$ are the ionization functions for each species of hydrogen and helium as a function of the redshift z . Combining this with dl :

$$dl = \frac{1}{1+z} \frac{c}{H_0} \frac{dz}{\sqrt{\Omega_m(1+z)^3 + \Omega_\Lambda}} \quad (6)$$

we get the expression for DM_{IGM} from eq.(2) as :

$$DM_{IGM}(z) = \frac{3cH_0\Omega_b f_{IGM}}{8\pi Gm_p} \times \int_0^z \frac{f_e(z)(1+z) dz}{\sqrt{\Omega_m(1+z)^3 + \Omega_\Lambda}} \quad (7)$$

for a flat Universe, where

$$\begin{aligned} f_e(z) &= (1-Y)\chi_{e,H}(z) + \frac{Y}{4}\chi_{e,He}(z) \\ &= (1-Y)\chi_{e,H}(z) + \frac{Y}{4}[\chi_{e,HeII}(z) + 2\chi_{e,HeIII}(z)] \end{aligned} \quad (8)$$

Here $\chi_{e,HeII}(z)$ and $\chi_{e,HeIII}(z)$ corresponds to the ionization functions of singly ionized Helium HeII and doubly ionized Helium HeIII respectively. We assume a sudden reionization occurring at z_r , and we express the ionization fraction of Helium as following equations:

$$\chi_{e,HeII}(z) = \begin{cases} 1, & \text{if } z > z_r \text{ (before HeII reionization)} \\ 0, & \text{if } z \leq z_r \text{ (after HeII reionization)} \end{cases} \quad (9)$$

$$\chi_{e,HeIII}(z) = \begin{cases} 0, & \text{if } z > z_r \text{ (before HeII reionization)} \\ 1, & \text{if } z \leq z_r \text{ (after HeII reionization)} \end{cases} \quad (10)$$

Before HeII reionization, all helium are singly ionized HeII, so $\chi_{e,HeII} = 1$ and $\chi_{e,HeIII} = 0$. After HeII reionization, all helium are doubly ionized HeIII, so $\chi_{e,HeIII} = 1$ and $\chi_{e,HeII} = 0$.

We assume all hydrogen atoms are ionized in our simulation scope, i.e. $\chi_{e,H}(z) = 1$.

3.1.2 Fluctuation of DM_{IGM}

In the above model, IGM is assumed to be even, ionized gas. In reality, large scale structures like galaxy filaments and halos exists, and bring in uncertainty in estimation of DM_{IGM} . From numerical simulation results, DM_{IGM} is obtained to be $\sim 280 \text{ pc cm}^{-3}$ at $z=1.5$ (Li et al. 2018b)(McQuinn 2014)(Faucher-Giguère et al. 2015).

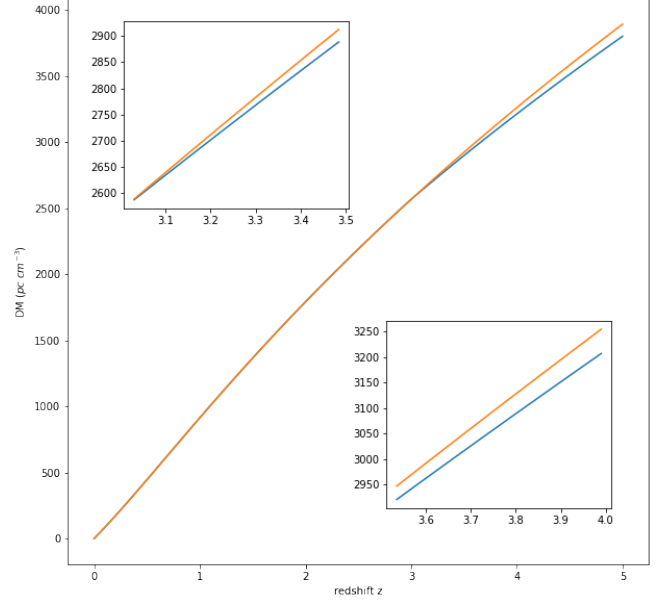


Figure 1. Plot of dispersion measure from IGM (DM_{IGM}) versus redshift. Blue line indicates HeII reionization happened at $z = 3$, red line indicates HeII reionization happened earlier than scope of plot, i.e. $z > 5$. Inset plots show same curve zoomed in at $z = 3$ to 3.5 and 3.5 to 4.

To propagate the uncertainty in DM_{IGM} to earlier Universe, we consider the variance of baryonic matter at different z . After ionization, we assume roughly all atoms in the hot intergalactic medium is ionized, so the electron density should be linearly related to the baryonic density n_{bar} . Therefore, we propagate the variance of DM_{IGM} at some z using a large scale structure simulation: the Millennium simulation project.

Statistically, $\sigma^2(\sum_i x_i) = \sum_i \sigma^2(x_i)$, if x_i are uncorrelated. For $DM_{IGM} = \int_0^z n_e/(1+z)dl$, the DM comes from integrating the electron density through the path of FRB signal travelled. Considering the FRB signal from $z > 3$, the distance from source to observer (Earth) is around 2 orders larger than the known large scale structures ($\sim 100 \text{ Mpc}$). Since the Universe is assumed homogeneous beyond scale of these structures, we can assume n_{bar} on the line of sight from the FRB to us is roughly uncorrelated.

Now we can write the variance of DM_{IGM} :

$$\begin{aligned} \sigma^2(DM_{IGM(z)}) &\propto \int_0^z \frac{\sigma^2(n_{bar})}{1+z} dl \\ &\propto \int_0^z \frac{\sigma^2(n_{bar})}{(1+z)^2 \sqrt{\Omega_m(1+z)^3 + \Omega_\Lambda}} dz \end{aligned}$$

From Millennium database: millimil simulation, we obtained the relative variance of baryonic matter from fitting as a function of z :

$$\sigma^2(n_{bar}) = 3.079e^{-1.429z} + 0.6597e^{-0.3328z} \quad (11)$$

Integrating gives

$$\begin{aligned} \frac{\sigma^2(DM_{IGM(z=3)})}{\sigma^2(DM_{IGM(z=1.5)})} &= 1.021 \text{ and} \\ \frac{\sigma^2(DM_{IGM(z=6)})}{\sigma^2(DM_{IGM(z=1.5)})} &= 1.025. \end{aligned}$$

This tell us that the $\sigma(DM_{IGM})$ is roughly constant at 280 pc cm⁻³ after $z = 1.5$.

3.2 DM Contribution by host galaxy disk

From the observed FRB DM which is greater than the foreground DM, it is understood that their origin is extragalactic. Thus the estimation of the contribution by the host galaxy in the overall DM budget is necessary. (Xu & Han 2015) have shown that depending on the type of the galaxy as hosts, the peak DM contribution could vary between few thousands (edge-on spiral galaxy) of pc cm⁻³ to few tens (dwarf and elliptical galaxies) of pc cm⁻³. Additionally, based on the the inclination angle of the host galaxy the line of sight of the incident FRB will vary and hence plays an important role in the host galaxy DM contribution.

3.2.1 Galaxy types

Host galaxies to FRB's could be modelled based on either, spiral, elliptical or dwarf galaxies. However knowledge of dwarf and elliptical galaxies in terms of their electron densities are not well modelled. Also, presence of local high density clump like regions within a galaxy can enhance the DM contribution from the host galaxies, should the line of sight propagate through such regions. Such clumps could be linked to HII regions. Such HII regions are scarcely observed in elliptical galaxies in comparison to the arms of the spiral galaxies (Zhou et al. 2014; Hou & Han 2014). In this analysis, we have used spiral galaxies as a result to model for the host galaxy DM contribution. For DM contribution from the elliptical or dwarf galaxies one can consult (Xu & Han 2015). Based on simulations with 10,000 FRB's they showed that for spiral galaxies the peak DM contribution can be of $\mathcal{O}(10^3)$ at high inclination angle ($>70^\circ$), while for elliptical and dwarf galaxies on average the peak DM contribution is 37 pc cm⁻³ and 45 pc cm⁻³ as a function of the inclination angle between $[0, \pi/2]$ respectively.

3.2.2 Galaxy database as reference

For our analysis, in order to model the host galaxy DM we used the data from the SPARC database (Lelli et al. 2016). From this database, we used the maximum disk data compiled from 175 galaxies by (Starkman et al. 2018). The scale length (R disk) measured at 3.6 micron band by the Spitzer and the baryonic mass are specifically used.

3.2.3 DM model of disk galaxies

To model the host galaxy DM, using a spiral galaxy model, we used the distribution function presented by (Xu & Han 2015). According to them the behaviour of the DM follows a skewed Gaussian distribution, given by :

$$\frac{dN}{dDM} = N_0 e^{-\frac{(DM-\xi)^2}{2\omega^2}} \int_{-\infty}^{\alpha\left(\frac{DM-\xi}{\omega}\right)} e^{-\frac{t^2}{2}} dt, \quad (12)$$

the parameters in the equations bear the usual representations as mentioned in the original paper. We used this distribution function (equation 12) together with the SPARC data mentioned above. For computing the parameters, ξ, ω, α we

further made use of the values mentioned in the table 1 of (Xu & Han 2015). We obtained the following fit values,

$$\xi = 66.52 \times \left[e^{-\left(\frac{(i-90)}{21.02}\right)^2} \right] + 27.56 \times \left[e^{-\left(\frac{(i-90)}{114.4}\right)^2} \right] \quad (13)$$

$$\omega = 35.36 \times \left[e^{(0.009625i)} \right] + 0.004973 \times \left[e^{(0.1266i)} \right] \quad (14)$$

$$\alpha = 3.003 \times \left[e^{-0.0008232i} \right] + 1.54e - 15 \times \left[e^{(0.3867i)} \right] \quad (15)$$

the viewing angle, i , is then randomly generated from a flat distribution of 0 to 90 degree.

3.2.4 Correction factors

In the above model, a Milky Way like galaxy (they adopted size and mass of Milky Way, with small scale structure neglected) is used to simulate the DM of interstellar medium within galactic disk. Milky Way own 3.6 μm scale length of 3.6 kpc and a baryonic mass of $\sim 1.2 \times 10^{11} M_{sun}$. To make the model for various disk galaxies, we consider a correction factor as follow.

Assume mean electron density is directly correlated with baryonic density within a galaxy, and all disk galaxies share same shape as milkyway as a simplified model, $\langle n_e \rangle \propto m/r^3$, n_e should have a correction factor of

$$\frac{m}{m_{MW}} \left(\frac{r_{MW}}{r} \right)^3 = \frac{m}{1.2 \times 10^{11}} \left(\frac{3.6}{r} \right)^3. \quad (16)$$

From eq.(4) $DM = \int_0^z n_e / (1+z) dl$. , We should consider an additional factor of r for DM since the path length of FRB signal travelling inside the galaxy disk is also affected by size of galaxy. In total we need to multiply the DM from above model by a factor of

$$\frac{m}{m_{MW}} \left(\frac{r_{MW}}{r} \right)^3 \left(\frac{r}{r_{MW}} \right) = \frac{m}{1.2 \times 10^{11}} \left(\frac{3.6}{r} \right)^2. \quad (17)$$

3.3 DM Contribution by local environment of FRB

3.3.1 Giant star forming regions

Recently, a non-repeating FRB, 180916.J0158+65, is localized to a star forming region inside spiral arm of a nearby spiral galaxy (Marcote et al. 2020). FRB 181112 is also located to a active star forming galaxy (Prochaska et al. 2019). A research on 21 FRBs show that the host galaxies contribute a large mean DM of ~ 270 pc cm⁻¹ (Yang et al. 2017), which possibly comes from nearby plasma like star forming HII regions. It is reasonable to assume a significant portion of FRBs to correlate with active star forming regions, especially the giant HII regions

3.3.2 HII region model in spiral galaxy

To estimate possible contribution of DM by host galaxy, we construct a simplified model in which the FRB is embedded in a HII region, and DM_{host} is completely contributed by the free electrons within the HII region. Since the shape and electron density distribution of the HII region is unknown, we

assume a spherical, homogeneous HII region for estimation. Recalling eq.(7), since the size of HII region is negligible in cosmological scale, we can assume the redshift, z , as constant and rewrite the equation as

$$DM_{\text{host}} = \frac{1}{1+z} \times \langle n_e \rangle \times P_L \quad (18)$$

Where $\langle n_e \rangle$ is the mean electron density in the HII region and P_L is the path length of FRB pulse travelled inside the HII region.

The electron density n_e can vary in different HII region. To estimate this term, we reference to a research on size and electron density of HII regions in nearby galaxy M51 (Gutiérrez & Beckman 2010). We found a general form of HII region mean electron density from fitting the data in M51 model:

$$\langle n_{e,M51} \rangle = \begin{cases} 45.8e^{-r/h} R^{-0.55} \text{ cm}^{-3}, & r < 1.4\text{kpc or } 4.6\text{kpc} \\ 28.9R^{-0.55} \text{ cm}^{-3}, & r \in [1.4, 4.6]\text{kpc} \end{cases} \quad (19)$$

Here h represents the scale length of the galaxy in kpc from fitting, r represents the distance of HII region from the center of the galaxy in kpc, and R represent the equivalent radius of the HII region in pc. In the paper, $h \sim 10$ kpc for M51, which match its neutral hydrogen scale length (Gutiérrez & Beckman 2010).

In this paper, we modelled our FRB's host galaxies based on the M51 model and therefore we use the same model for fitting. In the galaxy's database, we get the scale length of various galaxies at infrared ($3.6\mu\text{m}$) band, which mainly represents the stellar mass instead of neutral hydrogen. The M51 $3.6\mu\text{m}$ scale length is measured in (Leroy et al. 2008a) as 2.8kpc instead of 10kpc of its neutral hydrogen scale length. To account for this difference, we multiply the scale length by a factor of

$$\frac{\text{M51 } 3.6\mu\text{m scale length}}{\text{M51 neutral hydrogen scale length}} = 0.28 \quad (20)$$

To calibrate the effect of varying density in each galaxy, the electron density is also multiplied by a density factor of m/r^3 like in section §3.2.4. Here we take the baryonic mass of M51 (HI, HII and stellar mass) as $5 \times 10^{10} M_{\text{sun}}$ from (Walter et al. 2008), (Leroy et al. 2008b) and (Hughes et al. 2013). The overall HII region electron density is modelled as follow:

$$\langle n_e \rangle = \begin{cases} 45.8e^{-(r/0.28r_{\text{char}})} R^{-0.55} \frac{m}{5 \times 10^{10}} \left(\frac{2.8}{r_{\text{char}}} \right)^3, & \text{if } \frac{2.8r}{r_{\text{disk}}} < 1.4\text{kpc or } > 4.6\text{kpc} \\ 28.9R^{-0.55} \frac{m}{5 \times 10^{10}} \left(\frac{2.8}{r_{\text{char}}} \right)^3, & \text{if } \frac{2.8r}{r_{\text{char}}} \in [1.4, 4.6]\text{kpc} \end{cases} \quad (21)$$

Here r_{disk} refers to the scale length of the spiral galaxy at $3.6\mu\text{m}$ in kpc, m refers to mass of galaxy in M_{sol} . As above, r represents the distance of HII region from center of galaxy in kpc, and R represent the equivalent radius of the HII region in pc.

From the above assumption, we can randomly generate the DM_{host} distribution of FRBs with known redshift z . Observing data in (Álvarez-Álvarez et al. 2015), (Mayya 1994) and (Arsenault et al. 1988), radius R of giant HII regions in

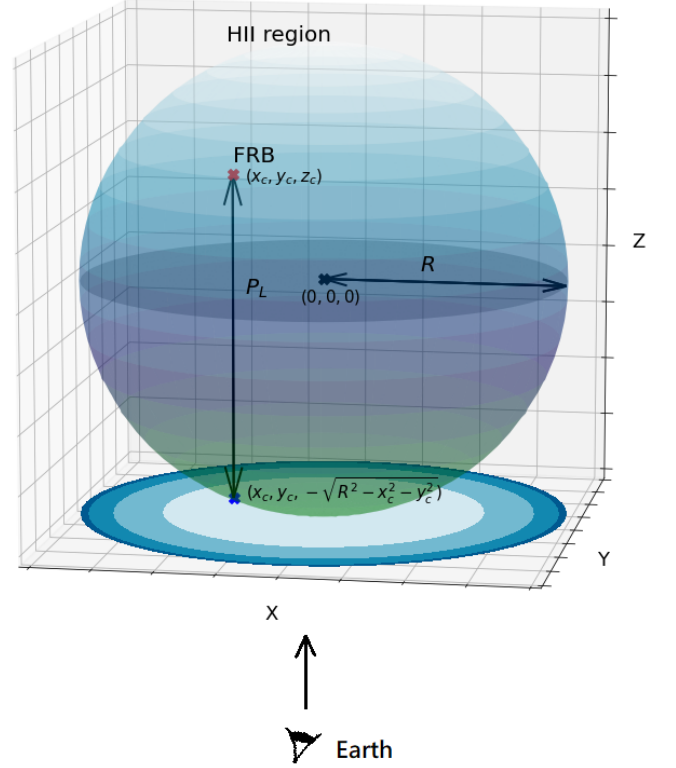


Figure 2. Model of FRB embedded in HII region and the projected path length of the signal travelled inside the HII region, P_L . Red cross represents FRB, blue cross represents the corresponding point on surface of spherical HII region. Earth (observer) is along the $+z$ direction

nearby galaxies has a log-normal like distribution,

$$R \sim 10^{N(\mu=2.1, \sigma^2=0.09)} \quad (22)$$

where N represents the usual normal distribution. For generation of r i.e. the position of HII regions from the center of the galaxy, we use an absolute normal distribution of $\left| N(\mu = 0, \sigma^2 = r_{\text{disk}}^2) \right|$, motivated by the fact that r_{disk} is the scale length of the galaxy in $3.6\mu\text{m}$ which represents mainly stars and dust.

After this, we need to know the path length l of the FRB signal travelled inside the HII region.

Assuming that the FRB is generated in an uniform random position inside a spherical HII region, the path length of FRB signal travelled inside the HII region l , is calculated by

$$P_L = z_c + \sqrt{R^2 - x_c^2 - y_c^2} \quad (23)$$

Where (x_c, y_c, z_c) is the coordinate of FRB with respect to the center of HII region, in pc, and R is the radius of the HII region. The equation follows a simple geometric model, shown in figure 2:

By running the above model from section 3.2 and 3.3, we obtained a heavy tailed contribution of DM host galaxy and FRB local environment with mean of $\sim 275 \text{ pc cm}^{-3}$, which agreed with the observed value of 270 pc cm^{-3} from 21 known FRBs (Yang et al. 2017). The corresponding variance can reach upto $\sim 390 \text{ pc cm}^{-3}$ from these terms.

For a FRB at redshift z , the expected contribution of $DM_{\text{HII}} + DM_{\text{GalaxyDisk}} = 275 \text{ pc cm}^{-3}/(1+z)$.

3.4 DM Contribution by Milky Way and nearby Universe

We also calculate the foreground contribution from the Milky Way's disk and spiral arms using the widely-used **YMW16** distribution (Yao et al. 2017). YMW16 is a model for the distribution of free electrons in the Milky Way, Magellanic Clouds and nearby IGM. The model is constructed based on DM measurement on radio pulsars. This model gives a good description of the Milky Way structure including the spiral arms and central bulge. The model also includes some known HII regions in our galaxy, like the Gum Nebula (Brandt et al. 1971), Galactic Loop I (Berkhuijsen et al. 1971) and the Local Bubble (Cox & Smith 1974). Figure 3 shows calculated DM for Milky Way from the earth using YMW16 electron density model. Therefore, we can deduce DM_{MW} later from our total DM to locate FRB to fair resolution.

3.5 Overall DM and the Variance

From the above model in section 3.1, 3.2 and 3.3. The overall DM of FRB are simulated as follow graph, with 1000 fictitious FRBs plotted (figure 4).

4 FITTING OCCURRENCE OF HEII REIONIZATION WITH SIMULATED FRB DM AND ITS VARIANCE

With the simulated FRBs versus redshift (z) distribution, along with the availability of the models of the individual DM components, we can now statistically analyse the number of FRB in range of $z = 3$ to 4 needed to constraint the epoch of HeII reionization.

We generate sets of synthetic FRBs with DM uncertainty generated from the above model, then fit them back to the ideal DM_{IGM} model as described in section 3.1.1. (DM_{host}) of 275 pc cm^{-3} is deduced from data to calibrate the effect of DM_{host} . The synthetic FRBs are grouped into bins of various sizes, so we can analysis the effect of the accuracy of fitting as a function of the number of FRBs observed. Additionally we also consider the error in the measured redshift of each FRB. We introduced a Gaussian uncertainty in redshift measurement z_{FRB} from 0% to 20% level, i.e. $\sigma(z_{\text{FRB}}) = G \times z_{\text{FRB}}$, where G range from 0% to 20%.

Standard deviation of $z_{r,\text{fit}}$, $\sigma(z_{r,\text{fit}})$ is obtained from the fitting, where $z_{r,\text{fit}}$ is the redshift of HeII reionization epoch obtained from the fit and the corresponding $\sigma(z_{r,\text{fit}})$ is the associated uncertainty. A smaller $\sigma(z_{r,\text{fit}})$ means that we have higher confidence on HeII reionization happening at $z_{r,\text{fit}}$. Taking a ground truth value of HeII reionization happening at $z = 3$, the uncertainty $\sigma(z_{r,\text{fit}}) = \epsilon$ then tells us that there is a $1 - \sigma$ confidence from the fit that HeII reionization happened in the neighbourhood of $z = 3.0 \pm \epsilon$.

Number of FRB detected	$\sigma(z_{\text{FRB}})$	$\sigma(z_{r,\text{fit}})$
10	0	1.47
	10%	1.54
	20%	1.78
100	0	0.500
	10%	0.515
	20%	0.602
1000	0	0.102
	10%	0.114
	20%	0.156

Table 1. Table summarizing the effect on the constraint of HeII reionization uncertainty level as a function of the FRB statistics and the redshift uncertainty. We present scenarios with three different levels of uncertainty fraction in the measured redshift, $\sigma(z_{\text{FRB}}) = [0, 10\%, 20\%]$ of the FRBs for each of the three cases of [10, 100, 1000] FRB detections. It is clear, at this level, we require $\mathcal{O}(10^2)$ FRBs for a detection of HeII reionization around the neighbourhood of $z \sim [3 - 4]$.

5 DISCUSSION

From the figure 5, we can see the $1 - \sigma$ constraint, $\sigma(z_{r,\text{fit}})$, tightens when number of FRBs increase (left to right variation along the x-axis). While the effect of increasing the noise in measured redshift of each FRB (vertical trend) is sub dominant.

In figure 6, we plot the HeII reionization detection uncertainty as a function of the number of FRBs detected, while assuming no error in redshift measurement. It is seen that we can constrain the HeII reionization to an uncertainty level of $\sigma(z_{r,\text{fit}}) < 0.5$ for $N_{\text{FRB}} \geq 100$ detected. Therefore, to obtain a fair constrain on the HeII reionization, we need hundreds of FRBs detected in $z = 3$ to 4.

We also show the sole effect on HeII reionization detection from the redshift measurement uncertainty by fixing the number of FRBs detected at 100. We can investigate the effect of uncertainty in redshift measurement ($\sigma(z_{\text{FRB}})$) in the detection, as shown in figure 7. We can see that $\sigma(z_{\text{FRB}})$ starts to effect the fitting results when it reaches $\sigma(z_{\text{FRB}}) = 6\% \times z_{\text{FRB}}$ (x axis, figure 7). $\sigma(z_{r,\text{fit}})$ grow from 0.5 to 0.6 when a percentage noise is turned up from 6% to 20%.

Similar effect is observed when we push the detected FRBs to 1000, as shown in figure 8. $\sigma(z_{r,\text{fit}})$ grow from 0.1 to 0.16 when a percentage noise of 20% is introduced to $\sigma(z_{\text{FRB}})$.

6 CONCLUSION

In this paper, we presented a cosmological based model on constraining the HeII reionization redshift in range of $z = 3$ to 4 by detecting the dispersion measure of distant FRBs. The model considers contribution from uneven IGM distribution, a host galaxy of disk type and a FRB local environment of giant HII region. Data used includes the the millennium simulation project (Millimil database), electron density model of disk type galaxy was based on Milky Way measurement, HII region electron density model from observations, the simulated dispersion measure from host galaxy and local environment fits of the observed data from 21 FRBs.

Synthetic FRBs are generated with the above model in different batch sizes, assuming HeII reionization happens at

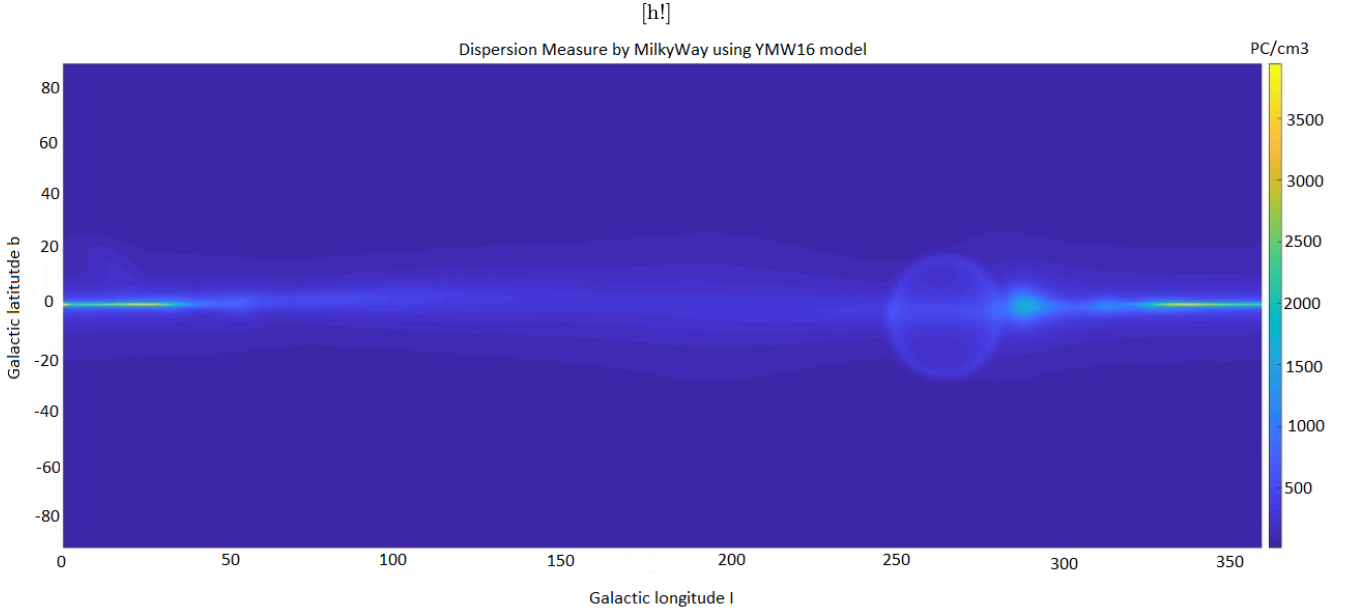


Figure 3. Calculated dispersion measure (DM) for Milky Way using YMW16 electron density model

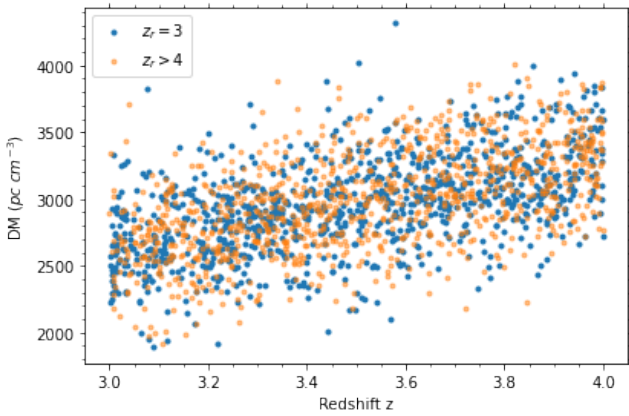


Figure 4. Dispersion Measure (DM) distribution as a function of the redshift, of the synthetic FRBs generated from the above model, in range of $z = 3$ to 4. The legends show the corresponding reionization redshift (z_r) assumed.

$z = 3$. To simulate real observations, we also considered redshift uncertainty $\sigma(z_{FRB})$ in the measurement of FRB, from 0 to 20% level of z_{FRB} following a Gaussian noise.

These FRBs are fitted to an ideal model of HeII reionization as mentioned in section §3.1.1 with least-square fitting.

From the fitting result, as shown in table 1, at least around a hundred FRBs in $z = 3$ to 4 is necessary to constrain the epoch of HeII reionization, $\sigma(z_{r,fit}) \sim 0.5$. With the addition of $\sigma(z_{FRB}) = 20\%z_{FRB}$, $\sigma(z_{r,fit})$ worsens to 0.6. For a larger population of 1000 FRBs measured, we can constraint $\sigma(z_{r,fit}) \sim 0.1$ ideally, and addition of $\sigma(z_{FRB}) = 20\%z_{FRB}$ worsens this to ~ 0.16 .

At the time of completion of this paper, we received an exciting news that a Milky Way soft gamma ray repeater (SGR), SGR 1935+2154, flared a FRB-like, double millisecond pulses with 30ms interval at 28 April 2020. Together

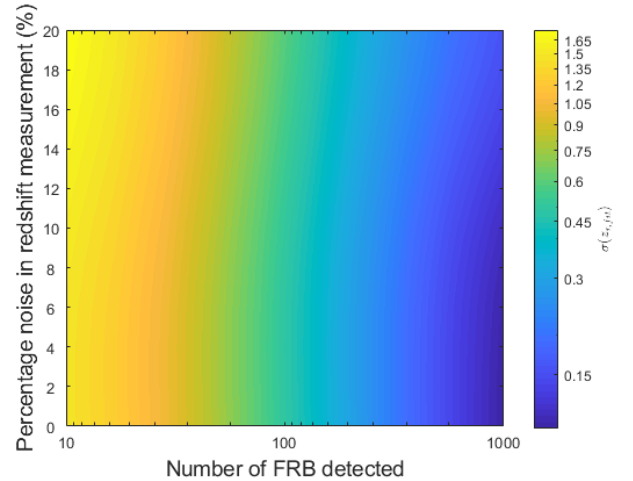


Figure 5. Joint plot showing the uncertainty in the HeII reionization detection as a function of both the FRB detection statistics and the associated % of noise in the corresponding redshift measurement.

there exist X-ray pulses arriving 8.63s earlier, completely match the delay brought by dispersion measure. This is the first time a FRB (or similar event) related to a known source, and provide us hints on possible origin of FRBs.

The estimation above is still valid since we assumed FRBs originated from source within galaxies, and correlated to young star / pulsar population. Also, SGR has possible correlation with star forming regions: SGR1806-20 is embedded in West-erhout 31, a star forming complex (Corbel et al. 1997). We hope to perform more detailed analysis in near future base on knowledge on magnetstars.

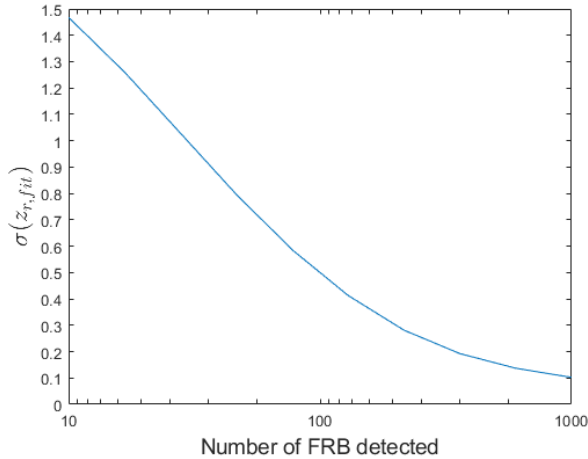


Figure 6. Figure showing the uncertainty level $\sigma(z_{r,fit})$ in the HeII reionization detection as a function of the FRB detection statistics. The above case is presented, while assuming there is no uncertainty involved in the redshift measurement.

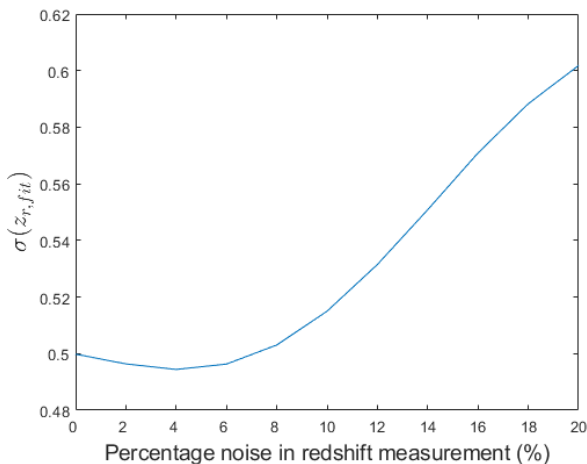


Figure 7. Plot showing the effect of redshift uncertainty (varied between 0 – 20%) on the HeII reionization detection for 100 detected FRB case.

7 ACKNOWLEDGEMENT

AM did this work with the grant from RK MES grant AP05135753, Kazakhstan.

REFERENCES

- Álvarez-Álvarez M., Díaz A. I., Terlevich E., Terlevich R., 2015, *MNRAS*, **451**, 3173
- Arsenault R., Boulesteix J., Georgelin Y., Roy J. R., 1988, *A&A*, **200**, 29
- Bandura K., et al., 2014, Canadian Hydrogen Intensity Mapping Experiment (CHIME) pathfinder. p. 914522, doi:10.1117/12.2054950
- Barkana R., Loeb A., 2001, *Phys. Rep.*, **349**, 125
- Berkhuijsen E. M., Haslam C. G. T., Salter C. J., 1971, *A&A*, **14**, 252

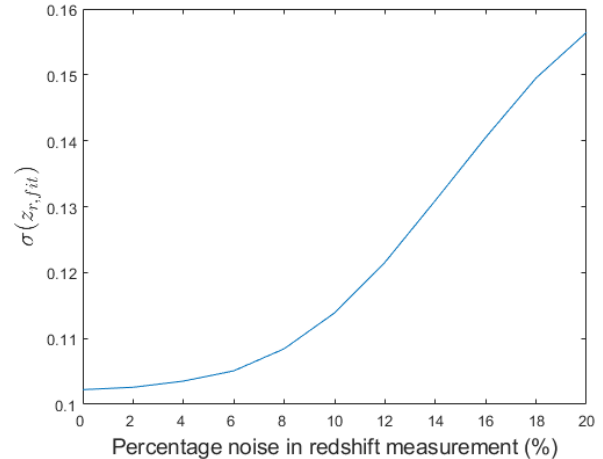


Figure 8. Plot showing the effect of redshift uncertainty (varied between 0 – 20%) on the HeII reionization detection for 1000 detected FRB case.

- Brandt J. C., Stecher T. P., Crawford D. L., Maran S. P., 1971, *ApJ*, **163**, L99
- Bromm V., Larson R. B., 2004, *Annual Review of Astronomy and Astrophysics*, **42**, 79
- CHIME/FRB Collaboration et al., 2019a, *Nature*, **566**, 235
- CHIME/FRB Collaboration et al., 2019b, *ApJ*, **885**, L24
- Caleb M., Flynn C., Stappers B. W., 2019, *MNRAS*, **485**, 2281
- Chatterjee S., et al., 2017, *Nature*, **541**, 58
- Corbel S., Wallyn P., Dame T., Durouchoux P., Mahoney W., Vilhu O., Grindlay J., 1997, *The Astrophysical Journal*, **478**, 624
- Cox D. P., Smith B. W., 1974, *ApJ*, **189**, L105
- Deng W., Zhang B., 2014, *ApJ*, **783**, L35
- Fan X., Narayanan V. K., Strauss M. A., White R. L., Becker R. H., Pentericci L., Rix H.-W., 2002, *AJ*, **123**, 1247
- Faucher-Giguère C.-A., Hopkins P. F., Kereš D., Muratov A. L., Quataert E., Murray N., 2015, *MNRAS*, **449**, 987
- Fukugita M., Hogan C. J., Peebles P. J. E., 1998, *ApJ*, **503**, 518
- Furlanetto S. R., Oh S. P., 2008, *ApJ*, **681**, 1
- Giroux M. L., 1990, in *BAAS*. p. 1306
- Gutiérrez L., Beckman J. E., 2010, *ApJ*, **710**, L44
- Hashimoto T., Goto T., Wang T.-W., Kim S. J., Wu Y.-H., Ho C.-C., 2019, *Monthly Notices of the Royal Astronomical Society*, **488**, 1908
- Hou L. G., Han J. L., 2014, *A&A*, **569**, A125
- Hughes A., et al., 2013, *The Astrophysical Journal*, **779**, 44
- Jaroszynski M., 2019, *MNRAS*, **484**, 1637
- Katz J. I., 2016, *ApJ*, **818**, 19
- Lelli F., McGaugh S. S., Schombert J. M., 2016, *AJ*, **152**, 157
- Leroy A. K., Walter F., Brinks E., Bigiel F., De Blok W., Madore B., Thornley M., 2008b, *The astronomical journal*, **136**, 2782
- Leroy A. K., Walter F., Brinks E., Bigiel F., de Blok W. J. G., Madore B., Thornley M. D., 2008a, *AJ*, **136**, 2782
- Li Z.-X., Gao H., Ding X.-H., Wang G.-J., Zhang B., 2018a, *Nature Communications*, **9**, 3833
- Li Z.-X., Gao H., Ding X.-H., Wang G.-J., Zhang B., 2018b, *Nature Communications*, **9**, 3833
- Liddle A. R., 2003, *An introduction to modern cosmology*. Wiley
- Linder E. V., 2020, *Phys. Rev. D*, **101**, 103019
- Lorimer D. R., Bailes M., McLaughlin M. A., Narkevic D. J., Crawford F., 2007, *Science*, **318**, 777
- Marcote B., et al., 2020, *Nature*, **577**, 190
- Mayya Y., 1994
- McQuinn M., 2014, *ApJ*, **780**, L33

- McQuinn M., Lidz A., Zaldarriaga M., Hernquist L., Hopkins P. F., Dutta S., Faucher-Giguère C.-A., 2009, *ApJ*, 694, 842
- Muñoz J. B., Loeb A., 2018, *Phys. Rev. D*, 98, 103518
- Paoletti D., Hazra D. K., Fabio F., Smoot G. F., 2011, *arXiv:2005.12222*, 733, L24
- Peacock J. A., 1999, *Cosmological physics*. Cambridge University Press, <https://doi-org.ezproxy.library.uq.edu.au/10.1017/CB09780511804533>
- Prochaska J. X., et al., 2019, *Science*, 366, 231
- Schnitzeler D. H. F. M., 2012, *MNRAS*, 427, 664
- Shull J. M., Smith B. D., Danforth C. W., 2012, *ApJ*, 759, 23
- Sokasian A., Abel T., Hernquist L., 2002, *MNRAS*, 332, 601
- Spitler L. G., et al., 2016, *Nature*, 531, 202
- Starkman N., Lelli F., McGaugh S., Schombert J., 2018, *MNRAS*, 480, 2292
- The CHIME/FRB Collaboration et al., 2020, arXiv e-prints, p. [arXiv:2001.10275](https://arxiv.org/abs/2001.10275)
- Thornton D., et al., 2013, *Science*, 341, 53
- Vishniac E. T., 1987, *ApJ*, 322, 597
- Walter F., Brinks E., De Blok W., Bigiel F., Kennicutt Jr R. C., Thornley M. D., Leroy A., 2008, *The Astronomical Journal*, 136, 2563
- Wiklind Tommy B. M., Volker Bromm e., 2012, *The first galaxies: theoretical predictions and observational clues*. Vol. 396, APS
- Worseck G., et al., 2011, *ApJ*, 733, L24
- Xu J., Han J. L., 2015, *Research in Astronomy and Astrophysics*, 15, 1629
- Yang Y.-P., Luo R., Li Z., Zhang B., 2017, *The Astrophysical Journal Letters*, 839, L25
- Yao J. M., Manchester R. N., Wang N., 2017, *ApJ*, 835, 29
- Yoshizawa A., 1978, *Journal of the Physical Society of Japan*, 45, 1019
- Zhou B., Li X., Wang T., Fan Y.-Z., Wei D.-M., 2014, *Phys. Rev. D*, 89, 107303